THE ASTROPHYSICAL JOURNAL, 209: 693–709, 1976 November 1

THE STRUCTURE OF ELLIPTICAL AND cD GALAXIES

AUGUSTUS OEMLER, JR.
Kitt Peak National Observatory* and Yale University Observatory
Received 1976 March 1; revised 1976 April 14

ABSTRACT

A method of photographic photometry is described which permits surface photometry of galaxies to be extended to very low ($S_v > 28$ mag arcsec^{-2}) surface brightnesses. It has been used to study elliptical galaxies in three clusters and a number of cD galaxies, with the following results. Ignoring flattening, elliptical galaxies form a one-parameter family with light distributions which are well described by an exponentially truncated Hubble law. Their limiting radii $R_1 \approx L_0^{2/3}$, where L_0 is an envelope-independent luminosity. There is no evidence that R_1 is determined by tidal interactions with other galaxies. The core radii of ellipticals decrease with decreasing luminosity, but make a sudden jump at $M_v \approx -15$.

The cD galaxies and other elliptical brightest cluster members appear to be very bright—but otherwise normal—giant elliptical galaxies with very diffuse, extended envelopes superposed. The extent and luminosity of these outer envelopes is a strong function of cluster richness; in the most extreme case the envelope extends to a radius of 2 Mpc. There appears to be some hope of explaining the occurrences and properties of cD galaxies by the effects of dynamical friction within clusters.

Subject headings: galaxies: formation — galaxies: photometry — galaxies: structure

I. INTRODUCTION

When compared with spiral and irregular galaxies, elliptical galaxies appear to be dull and uninteresting objects. Because of this, and because of technical difficulties in studying them, they have received much less attention than their more spectacular-looking relatives. However, their very simplicity makes them attractive first subjects in any attempt to understand the formation and structure of galaxies. The largest available study of ellipticals is that by Liller (1960, 1966) of members of the Virgo cluster. Smaller studies have been made by van Houten (1961), by Markaryan, Oganesyan, and Arakelyan (1965) and by others. Unfortunately, none of the published photometry goes sufficiently deep to provide information on the outer envelopes of the galaxies. A number of theoretical models of ellipticals have been constructed in recent years (Gott 1975; Larson 1974*a*; Wilson 1975); a thorough study of their properties is, therefore, badly needed.

The related class of D galaxies was first defined by Morgan (1958) as one of the form families in his system of galaxy classification. The precise definition of the class has evolved somewhat; as stated most recently by Morgan, Kayser, and White (1975) a D galaxy is one "having an elliptical-like nucleus surrounded by an extensive envelope." Matthews, Morgan, and Schmidt (1964) found that one-half of all strong radio sources could be identified with a D-type galaxy which was the centrally located, outstandingly bright member of a cluster of galaxies. These galaxies they called cD's, meaning supergiant D galaxies.

The relationships between E galaxies and cD galaxies, and between cD galaxies and the compact, elliptical-rich clusters in which they are apparently always found (Oemler 1974), are quite interesting by themselves. They are also of interest because of the importance of these galaxies as standard candles in the usual cosmological tests (Sandage 1961; Gunn and Oke 1975). This paper presents a survey of the optical structure of elliptical and cD galaxies, using photometry of photographic plates. Because the results depend heavily on the ability to measure very low surface brightnesses and because the methods used are, I believe, superior to those used in previous work, they will be described in some detail in the next section. Description of the observations themselves begins in § III.

II. PHOTOGRAPHIC SURFACE PHOTOMETRY

a) Reduction Methods

A typical photographic plate contains a very large quantity of information, but techniques used in the past have been able to extract only a very small fraction. Isodensity tracings (see, for example, Kormedy and Bahcall 1974) can display the full two-dimensional content of a plate, but only in a semiquantitative form which is unsuitable for further analysis. Most quantitative work has been done by microphotometer tracings along a few lines through a galaxy image. While this method is completely satisfactory at high surface brightnesses, the extent to which one can use it to follow a galaxy is limited by three factors: grain noise, the envelopes of

* Operated by the Association of Universities for Research in Astronomy, Inc., under contract with the National Science Foundation.

neighboring stars and galaxies, and variations in plate sensitivity and fog. The procedures described below are designed to handle these factors in the most effective way.

The plate of each galaxy to be studied is scanned on a digitizing two-axis microdensitometer in a series of square rasters centered on the object. Each square, which is about 4 times larger than the next smaller, is digitized in either 100 × 100 square boxes or 1000 × 100 rectangular boxes, depending on the reduction method to be used. As many rasters are obtained as is necessary to both resolve all structure in the center and also extend well beyond the galaxy cutoff.

The 100 × 100 raster scans used for most of the ellipticals were cleaned by displaying the data on a computer graphics terminal and removing sections of the data surrounding stars, galaxies, plate defects, and other intruding objects. For the larger ellipticals and for all of the cD's, in whose extended envelopes field contamination is more important and for which higher accuracy was desired, 1000 × 100 raster scans were used and were cleaned by the following method. The distribution of the surface brightness of individual points around the mean of the sky is a Gaussian of standard deviation σ due to grain noise, with an additional high-surface-brightness tail due to stars and galaxies. The value of σ is first determined from a sample area of the raster scan. Now, each line of 1000 points is divided into 50 overlapping strings of 50 points each. A low-order least-squares fit is made to the run of surface brightness along each string, and all points in the central 20 which are more than 2.5 σ higher than the fit are rejected. After an entire line is processed, the procedure is iterated until no more points are rejected. If done with care, this method removes all small background objects without affecting the large-scale gradient in the envelope of the galaxy being studied. Some additional editing of the data by hand is sometimes necessary to remove the outer parts of a very large object. The final data are averaged into a 100 × 100 array. When either method is used, the level of the cleaning cutoff is set by grain noise and varies with plate type and scan size, but typically all points with surface brightness above sky of 26 visual mag arcsec^{-2} can be removed.

The cleaned data are now ready for analysis. The outermost five to 10 columns and rows of the data are used to determine the sky background. For those raster scans of the cD's and larger ellipticals which extend well beyond the edge of the galaxy, the sky level is fitted to a low-order two-dimensional polynomial following the criteria for stability of Jones *et al.* (1967). All other raster scans are assigned an approximate constant background value, which is corrected when the galaxy profile is obtained.

After correction for background, only galaxy light remains. The center of the galaxy is found from the position of the brightest point, or from the centroid of such points if the image is saturated. All of the analysis after this point assumes that the isophotes of the galaxy are concentric ellipses with the same orientation. Now, 50 rays are drawn from the center at equal angular intervals, and the radii along each ray corresponding to a series of surface brightnesses (usually at 0.3 mag intervals) are tabulated out to some limiting surface brightness. From these data the position angle of the major axis and the axial ratio of each isophote are determined. A least-squares fit is made to the run of axial ratio b/a with semimajor axis a; beyond that limiting surface brightness, typically $S_v = 26$ mag arcsec^{-2}, where the data become too noisy to determine it directly, a constant axial ratio is assumed equal to that of the last measured point. Using the parameters just obtained, a series of ellipses is constructed from the center of the galaxy to the edge of the data grid. Finally, by averaging the surface brightness around each ellipse, the run of surface brightness with radius, defined as $r = (ab)^{1/2}$, is obtained.

The greatest problem affecting most published surface photometry is systematic errors in the faint outer parts of the galaxy profile due to uncertainty in the sky background level. In order to minimize this problem, all profiles have been followed out for at least a factor of 2 in radius beyond the last detectable point in the galaxy.

The galaxy profiles obtained by the procedure described above make efficient use of the data available on a photographic plate, and permit photometry to be extended to quite low surface brightnesses. The major sources of error are incorrectly subtracted background variations, incompletely removed envelopes of neighboring stars and galaxies, and errors in the characteristic curve of the photographic plate. A number of tests have been performed to estimate these errors, and they are described below.

b) *Accuracy of the Photometry*

Four 098 plates of NGC 4839, the third brightest galaxy in the Coma cluster, each with its own sensitometric calibration, were obtained on the Palomar 48 inch (1.2 m) Schmidt telescope. Each plate was measured and reduced separately, and four profiles were obtained. These were averaged to obtain a mean profile to which the individual profiles were compared. The standard deviation of the individual profiles about the mean is shown, as a function of surface

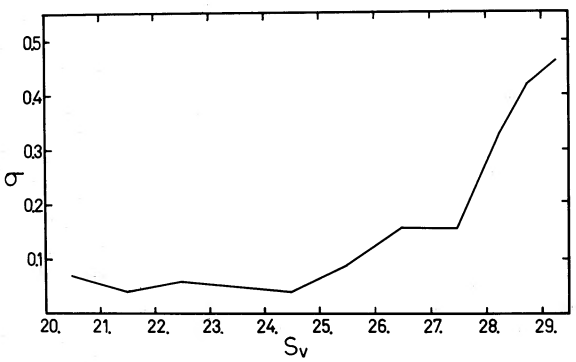

FIG. 1.—The standard deviation, in magnitudes, of surface brightness measurements of NGC 4839, as a function of surface brightness.

brightness, in Figure 1. These results can be represented by

$$\sigma = 0.05S_{\rm gal} + 7 \times 10^{-4}S_{\rm sky}\,, \qquad (1)$$

the sky brightness in the V-band being about 22 mag arcsec^{-2}.

The surface brightness distribution in M87 has been measured by a number of workers. The profile obtained in this study will be presented in § III, but the deviations from it of other published profiles are shown in Figure 2. The zero point of the magnitude scale of each set of observations has been adjusted to give the best overall agreement. Only the profile by de Vaucouleurs (1969), obtained from photoelectric drift scans, extends as far as the one presented below. De Vaucouleurs could not properly determine the sky background, and had to guess. The higher open circles are the profile resulting from his guess for background; the lower open circles come from another guess within his stated uncertainties. The agreement of the latter points is much better, but still unsatisfactory. However, it is straightforward to calculate, from the information presented in his paper, what the noise in de Vaucouleurs's profile should be, due to photon statistics and contamination by faint stars and galaxies. One finds that the uncertainty in the outer points of his profile is equivalent to $S_v \approx 27.5$ mag arcsec^{-2}, which is quite sufficient to reconcile the two profiles. Liller's photometry shows systematic deviations at both large and small radii which are probably due to the calibration error discovered by van Houten (1961). With these few exceptions, all of the data agree among themselves and agree with the newly measured profile with a standard deviation of 0.13 mag within the interval $17.0 < S_v < 24.0$.

The images of a number of galaxies in the Coma cluster were measured on a long-exposure 10 × 10 inch (25 × 25 cm) Schmidt telescope plate, and on short- and long-exposure plates obtained at the prime focus of the KPNO 4 m telescope. With one exception, all sections of all of the profiles agreed among themselves and agreed with electronographic and photoelectric photometry by Ables and Ables (1972) and by Rood and Baum (1968) to better than 0.1 mag for $S_v < 25$ mag arcsec^{-2}). The exception was the high-surface brightness ($S_v < 21.5$ mag arcsec^{-2}) ends of the Schmidt profiles, which were systematically in error. Examination of other photometry showed that this was a general property of 10 × 10 inch Schmidt telescope plates. Because of the method by which these plates are coated, the emulsion is thinner near the edges, where the calibration spots are located, than over the rest of the plate. The resulting error in the plate's characteristic curve is important only at high densities, and has been corrected in the photometry described in § III. However, it is possible that systematic errors as large as 0.15 mag remain at the bright end of some of the profiles.

The comparisons discussed above allow us to estimate all errors caused by plate imperfections and poor fits to the isophotes by the reduction routines. The only important error left is that due to neighboring stars and galaxies which can, of course, repeat from measurement to measurement. This is most important for the centrally located cD galaxies, whose extended envelopes overlie the general galaxy distribution in their clusters. If most cluster members had large, overlapping envelopes, one could make very serious errors while trying to measure the amount of light belonging to the envelope of the central galaxy itself. Fortunately, this is not the case. The galaxy profiles presented in § III show that only a few percent of the light of most galaxies is located beyond the 26 mag arcsec^{-2} isophote, where it will be missed by the cleaning procedures. On the other hand, the surface brightness of the envelope of the cD galaxy in Abell 2670, a typical case, is at all radii about one-half

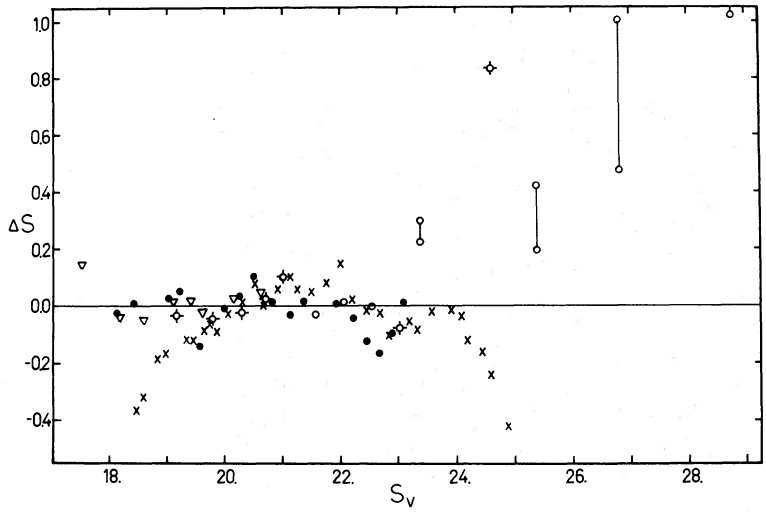

FIG. 2.—The deviation of the profile of M87 measured here from other published measurements. *Triangles*, van Houten (1961); *crosses*, Liller (1960); *filled circles*, Markaryan *et al.* (1965); *open circles*, de Vaucouleurs (1969); *circled points*, Baum, reported in Liller (1966).

that which would be produced by the smeared-out light of all of the other cluster members (Oemler 1973). Thus the total contribution of the light of other galaxies to the meaured profile of the cD galaxy should be considerably less than 10 percent and thus negligible.

We may form a reasonable estimate of the accuracy of the profiles presented below. For those large galaxies cleaned by the more thorough method,

$$\sigma = 0.1\, S_{\rm gal} + 0.001\, S_{\rm sky}\,; \qquad (2)$$

and for all others,

$$\sigma = 0.1\, S_{\rm gal} + 0.0014\, S_{\rm sky}\,, \qquad (3)$$

where again, $S_{\rm sky} \approx 22$ mag arcsec^{-2}.

III. OBSERVATIONS OF E AND cD GALAXIES

Plates for this study were obtained on the Palomar 48 inch (1.2 m) Schmidt and KPNO 4 m telescopes. Several combinations of plates and filters were used. All Schmidt telescope plates were in one of two bands: J, a band centered at 5000 Å and produced by a combination of J plate and Wratten 4 filter, or F, a band centered at 6500 Å and produced by a combination of a 103a-F, 098, or 127 plate behind a RG 610 filter. A description of this photometric system may be found in Oemler (1974). All KPNO 4 m exposures were on IIIa-J plates behind a GG 385 filter, producing a broad blue-green band extending from 3900 to 5400 Å. With the exception of one short-exposure 4 m telescope plate of the center of the Coma cluster kindly provided by Dr. Stephen Strom, all were deep exposures with $0.4 < D_{\rm sky} < 1.0$.

To make the results more accessible, all photometry has been reduced to the V band. Absolute calibrations have been obtained from diverse sources, as described below for the individual objects. It is unlikely that this hodgepodge of photometric systems has degraded the results, which were not intended to provide absolute photometry more accurate than 0.1 mag. The following relations have been used to reduce the data to the V band:

$$J - V = 0.3\,, \qquad V - F = 0.8. \qquad (4)$$

Most of the elliptical galaxies studied were obtained from fields near three clusters: Coma, Perseus, and Abell 1314. KPNO 4 m telescope plates covering the center of Coma out to a radius of 1° were searched for as many ellipticals as possible over as wide a brightness range as possible. Outside this area, ellipticals were found using a 10 × 10 inch Schmidt telescope plate, which did not allow identifications to as faint a limit. All Coma galaxies except NGC 4839 were measured on a IIIaJ Schmidt telescope plate. As discussed in § II*b*, the profile of NGC 4839 was obtained from four red Schmidt telescope plates. Absolute calibration of the Coma photometry is based on the photoelectric photometry of Rood and Baum (1968) and on the photographic photometry in Oemler (1974). Elliptical galaxies in the Perseus cluster were selected and measured on a very deep 10 × 10 inch IIIaJ Schmidt telescope plate. Absolute calibration is based on Sandage's (1972*c*, 1973) photoelectric photometry of NGC 1275. The profiles of Perseus cluster galaxies are somewhat noisier than usual because of the very high density of foreground stars in this region of the sky. Galaxies in A1314 were identified and measured on a 5 × 7 inch IIIaJ Schmidt telescope plate. Calibration is based on photometry of the same galaxies in Oemler (1974).

A list of all galaxies for which measurements were completed is presented in Table 1. Galaxies are identified, in order of preference, by their NGC or IC numbers, by their designation in the *Catalogue of Galaxies and Clusters of Galaxies* (Zwicky *et al.* 1961–1968), or (in Coma) by the identifying numbers given by Rood and Baum (1967). Coma cluster galaxies with none of these designations are identified in Figure 3. Since some galaxies were rejected because of measurement problems, this is in no sense a complete list of elliptical galaxies in these clusters. The small numbers of galaxies in Perseus and A1314 reflect both their small populations of ellipticals and the difficulty in reliably identifying elliptical galaxies at these distances without the aid of large-scale plates.

All three clusters are so distant that only the cores of the very largest galaxies are resolved. In order to provide more information on the core sizes of ellipticals, published surface photometry, mostly by Liller (1960, 1966), of nearby galaxies has been used. These galaxies are listed in Table 2. Before use, Liller's photometry was corrected for the systematic error discussed in § II*b*. Also listed in Table 2 are a number of Local Group dwarf ellipticals studied by Hodge and others. Galaxies fainter than NGC 147 can be studied only by star counts. Surface densities of stars were converted to surface brightnesses by using Hodge's estimated absolute magnitudes, which are rather uncertain.

The selection of brightest cluster members for study was neither systematic nor unbiased. Within the limitations of available plate material an attempt was made to include a representative sample of clusters whose brightest members ranged from extreme cD's to normal-looking ellipticals. A brief description of each galaxy chosen follows.

Morgan, Kayser, and White (1975) have published a list of suspected cD galaxies in small groups. Since all previous examples were located in rich clusters, these are significant objects if true cD's. NGC 4073 in the cluster MKW 4 is the only example for which good plate material could be obtained, provided by Stephen Shectman. Its profile was measured on one 10 × 10 inch IIIaJ Schmidt telescope plate. Absolute calibration is based upon the magnitude given by Zwicky *et al.* (1961–1968) and is uncertain by several tenths of a magnitude. The redshift of NGC 4073, also provided by Shectman, is 0.0193.

NGC 1275, the brightest galaxy in the Perseus cluster, is, of course, a very peculiar object, but its gross continuum light distribution is not atypical of giant ellipticals. Plate measurement and calibration was as described above for other Perseus ellipticals.

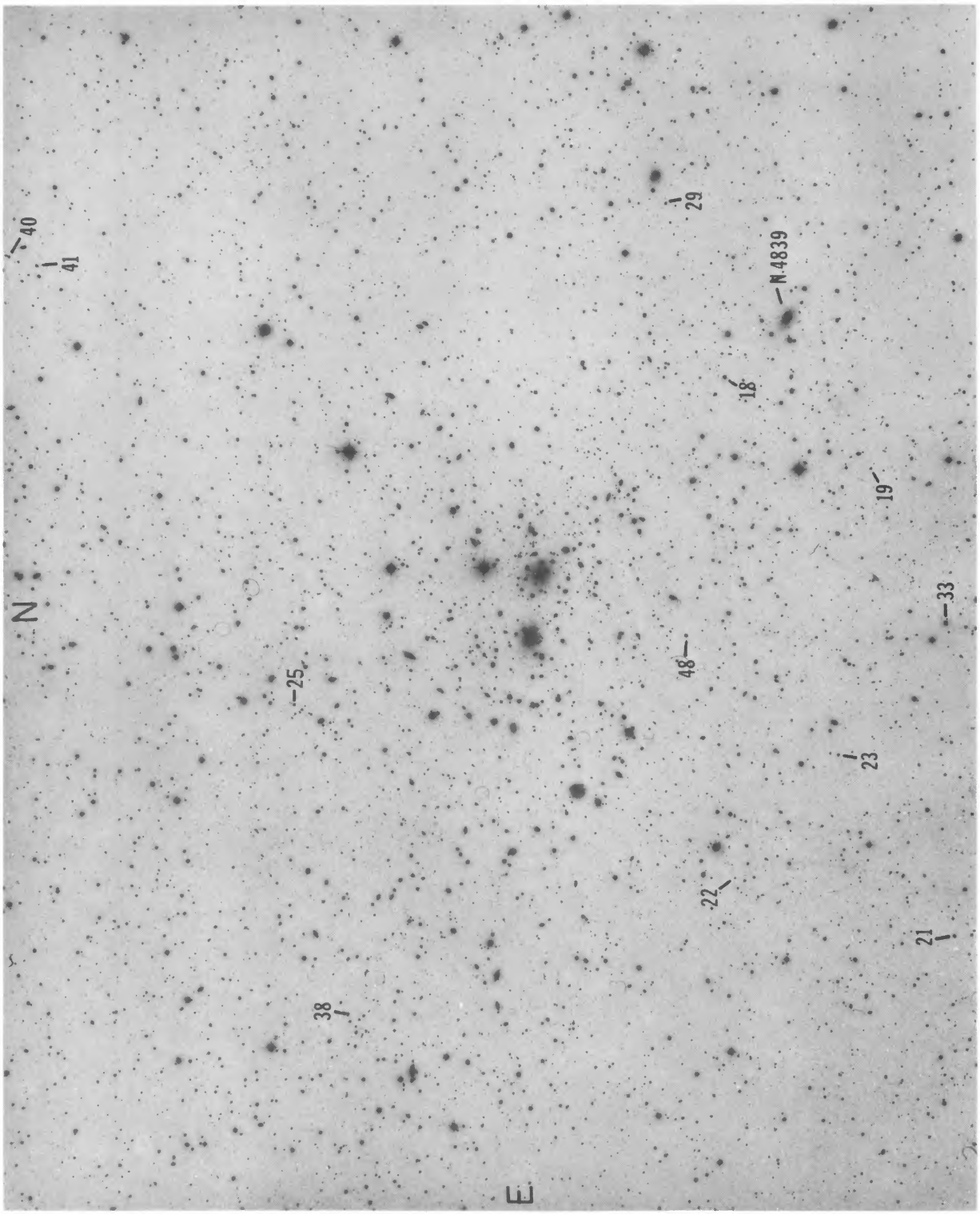

FIG. 3.—Faint elliptical galaxies in the Coma cluster.

TABLE 1

Elliptical Galaxies

Galaxy	M_V	M_o	logα	logβ	logR_1
Coma Cluster					
NGC 4816+	-23.22	---	---	---	2.16
NGC 4827	-22.82	-19.59	1.79	0.03	1.89
NGC 4839	-24.08	-20.40	---	---	2.75
NGC 4840	-21.87	-18.69	---	---	1.85
NGC 4841+	-23.11	-20.00	---	---	1.86
NGC 4864+	-21.98	---	---	---	1.55
NGC 4881	-22.14	-19.05	1.66	-0.11	1.90
NGC 4906	-21.59	-18.85	1.19	-0.07	1.40
NGC 4921	-22.05	-18.92	1.67	<-0.30	1.70
NGC 4926	-22.63	-19.54	1.72	<-0.10	1.82
NGC 4927	-22.49	-19.27	1.57	-0.16	1.71
NGC 4952	-22.79	-19.60	1.79	-0.17	1.87
NGC 4957	-22.66	-19.65	1.80	0.06	1.86
IC 832	-21.93	-18.91	1.56	-0.25	1.65
IC 842	-21.13	-18.25	1.42	-0.30	1.57
IC 3957	<-21.35	-17.64	>2.50	<-0.70	>1.87
IC 3959	<-21.96	-18.28	>2.50	<-0.70	>1.95
IC 4051	-22.34	-19.45	1.60	0.10	1.72
IC 4133	-21.29	-18.15	1.42	<-0.40	1.54
13 00.4+28 07*	-19.25	-17.69	0.82	0.14	1.09
13 03.0+29 34	-21.40	-18.21	1.45	-0.59	1.62
RB 31	-19.25	-17.20	0.78	-0.20	1.02
RB 129	-20.17	-17.27	1.20	<-0.60	1.40
RB 195*	-18.81	-16.74	0.73	-0.27	1.02
RB 224	-20.29	-17.80	0.92	-0.20	1.22
RB 241	-21.64	-18.55	1.47	<-0.30	1.67
RB 268	-21.41	-18.57	1.70	0.20	1.70
Coma 18	-20.76	---	---	---	1.65
Coma 19*	-19.54	-17.94	0.80	0.00	1.05
Coma 21	-20.56	---	---	---	1.25
Coma 22*	-18.66	-16.95	0.74	-0.04	0.94
Coma 23	-19.70	-17.06	1.12	-0.22	1.23
Coma 25	-19.28	-17.15	0.98	-0.25	1.10
Coma 29	-19.99	-17.22	0.85	<-0.50	1.10
Coma 33	-21.18	-18.10	1.45	-0.28	1.57
Coma 38	-19.75	-17.80	0.87	0.00	1.12
Coma 40	-19.80	-16.74	1.02	<-0.70	1.20
Coma 41	-19.89	-16.80	1.14	<-0.70	1.25
Coma 48	-20.29	-17.29	1.23	<-0.70	1.42
Perseus Cluster					
NGC 1265	-23.80	-20.85	1.80	<-0.10	1.98
NGC 1270+	-22.78	-19.60	---	<-0.40	1.69
NGC 1272+	-22.87	---	---	---	1.99
NGC 1273	-22.29	-19.25	1.54	<-0.40	1.72
NGC 1278	-23.02	-20.32	1.51	0.14	1.79
NGC 1282	-22.56	-19.40	1.72	<-0.40	1.82
NGC 1283	-21.27	-17.94	1.10	<-0.50	1.73
NGC 1293	-22.70	-19.28	1.86	<-0.50	1.92
IC 310	-22.99	-19.93	1.91	-0.15	2.00
3 14.6+14 16	-21.42	-18.39	1.32	<-0.50	1.46
3 15.6+41 34*	-20.82	-18.50	1.10	-0.20	1.40
3 15.9+41 31	-20.88	-17.80	1.12	<-0.50	1.58
3 16.2+41 27	-21.76	-19.10	1.27	<-0.40	1.52
Abell 1314					
IC 708	-23.46	-20.23	2.08	-0.10	2.12
IC 709	-22.79	-19.49	1.84	<-0.30	1.90
IC 711	-22.63	-19.21	1.79	<-0.60	1.93
11 33.8+49 24	-22.64	-19.47	1.80	-0.40	1.90
11 33.9+49 20	-22.30	-19.19	1.62	-0.45	1.76

* Poor fit. M_o very uncertain.

\+ Possible SO.

There is some uncertainty whether M87 or NGC 4472 is the largest galaxy in the Virgo cluster; M87 has been chosen here mainly because of the available plate material. Two 10 × 10 inch Schmidt telescope plates and one 4 m telescope plate were used to obtain the profile; absolute calibration is based on the photometry of Sandage (1973).

Abell 779 is a rather poor cluster dominated by one giant elliptical. NGC 2832 was measured on two Schmidt telescope plates; absolute calibration is based on Sandage's (1973) photometry.

The central galaxy in Abell 1413 was noted by Morgan and Lesh (1965) as perhaps the largest of all cD galaxies. Its profile was obtained from one 4 m telescope and two Schmidt telescope plates; absolute calibration is based on the photometry of Sandage (1972*a*). This, the largest galaxy studied, is the only one whose total extent is in serious doubt. Its profile was followed out to a radius of 24′, equal to 3.5 Mpc. At this point sky seems to have been reached; but because the profile could not be followed out further, there is some uncertainty.

Abell 2147 is a rather ill-defined entity, being part of the large cloud of galaxies which includes A2147, A2152, and the Hercules cluster. However, if it is a real cluster, there is no doubt which is its brightest member: a large elliptical belonging to a short chain of galaxies near its center. This galaxy's profile was measured on one Schmidt telescope plate and calibrated by using Peterson's (1970) photometry.

Abell 2162 is another rather poor cluster. NGC 6086 was measured on two Schmidt telescope plates and calibrated by using Peterson's (1970) photometry.

NGC 6166 in Abell 2199 is one of the type examples of cD's, as defined by Matthews, Morgan, and Schmidt (1964). In some aspects, though, it is an atypical and very peculiar object. Minkowski (1961) has published a good photograph of its core. Often called a multiple-nucleus galaxy, it consists of a large, diffuse core of peculiarly low central surface brightness with several small, high-surface-brightness objects superposed on it. It is impossible to tell whether these are secondary condensations within the core or merely normal small elliptical galaxies seen in projection against the cD. The profile of NGC 6166 was measured on two Schmidt telescope plates and calibrated by using Sandage's (1973) photometry.

NGC 7728 is a prominent cD in the rich cluster Abell 2634. Its profile was measured on two Schmidt telescope plates and calibrated by using JF band

TABLE 2

Data From Other Sources

Galaxy	M_V	M_o	logα	logβ	logR_1	Source
M32	---	-13.54	---	-1.90	---	1
NGC 147	-14.60	-13.82	---	-0.33	0.28	2
NGC 185	-15.30	-13.99	-0.06	-0.56	0.19	3
NGC 205	---	-14.05	---	-0.60	0.49	4
NGC 3379	-21.80	-18.53	1.47	-0.53	1.52	5,6
NGC 4168	---	-18.20	---	-0.06	---	8
NGC 4360	---	-17.00	---	-0.23	---	8
NGC 4365	---	-19.41	---	-0.08	---	7
NGC 4374	---	-19.64	---	-0.05	---	7
NGC 4435	---	-18.76	---	-0.08	---	8
NGC 4452	---	-19.10	---	-0.14	---	8
NGC 4459	---	-19.06	---	-0.05	---	7
NGC 4472	---	-20.74	---	0.02	---	7,9
NGC 4515	---	-16.85	---	-0.50	---	8
NGC 4649	---	-20.46	---	0.20	---	7
Draco	- 7.20	- 6.68	-0.53	-0.71	-0.32	10
Fornax	-13.60	-13.19	0.14	-0.08	0.35	11
Leo I	-11.40	-12.88	-0.50	-0.10	-0.20	12
Leo II	- 9.80	-10.39	-0.50	-0.34	-0.25	13
Sculptor	-10.90	-11.91	-0.42	-0.11	-0.09	14
Ursa Minor	- 7.20	- 6.95	-0.50	-0.67	-0.28	15

1. deVaucouleurs (1953)
2. Hodge (1974)
3. Hodge (1963b)
4. Hodge (1973)
5. Miller and Prendergast (1962)
6. Burkhead and Kalinowski (1974)
7. Liller (1960)
8. Liller (1966)
9. van Houten (1961)
10. Hodge (1964b)
11. Hodge and Smith (1974)
12. Hodge (1963a)
13. Hodge (1962)
14. Hodge (1961)
15. Hodge (1964a)

photoelectric photometry. Certain measurement problems prevent following its profile out as far as is desired; its total extent and luminosity are, therefore, slightly uncertain, due to a 0.2 percent uncertainty in the sky level.

The cD galaxy in Abell 2670 is another of the type examples of Matthews, Morgan, and Schmidt (1964). Its photometry is described in detail in Oemler (1973).

The profiles of a number of the brightest cluster members were measured in both the J and F bands. In no case was there any significant difference between the two, and they have always been combined. Correction for galactic absorption was made using Sandage's (1973) prescription. Conversion to absolute magnitude and corrections for cosmological and redshift effects have been made on the assumption that the Hubble constant $H_0 = 50$ km s^{-1} and the deceleration parameter $q_0 = 0.0$. Except for MKW 4 and A2670, redshifts of the clusters have been taken from Noonan (1973). All of the galaxy profiles presented below are given in terms of visual magnitude per square arc second versus a radius defined as the geometric mean of the semimajor and semiminor axes.

Figure 4 contains profiles of some of the elliptical galaxies which are typical of the sample as a whole. Figure 5 contains the profiles of all of the brightest cluster members plus that of NGC 4839. Radii in Figure 4 are in arc seconds; those in Figure 5 are in kiloparsecs. By integrating under the profiles, total magnitudes may be obtained. These are listed in column (2) of Tables 1 and 2 and in column (3) of Table 3, except for those galaxies studied by others whose photometry does not extend far enough to include all of the galaxy luminosity.

IV. ANALYSIS

a) Elliptical Galaxies

Inspection of the elliptical galaxy profiles shows that they are quite uniform in shape, as has been known since Hubble's (1930) original work. However, as has been known for a long time, the surface brightness law proposed by Hubble,

$$S = \frac{S_0}{(1 + r/\beta)^2}, \tag{5}$$

while accurately describing the cores of ellipticals, breaks down at large radii where the galaxy surface brightness falls more rapidly than an r^{-2} power law. Most of the profiles in Figure 4 show a luminosity gradient (in a log-log plot) which increases steadily with radius, although a few of the large galaxies have profiles with an inflection point at an intermediate radius.

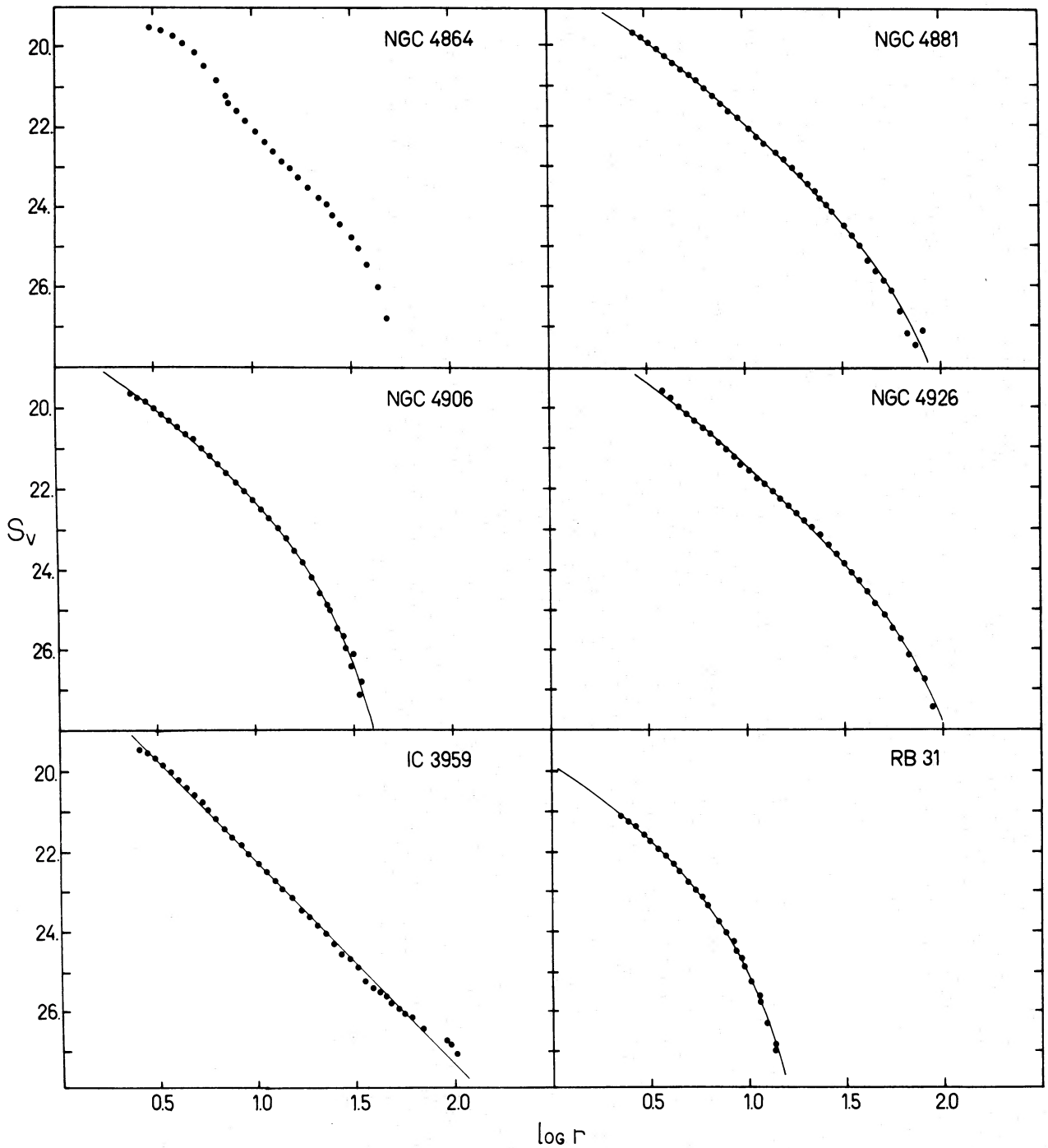

FIG. 4.—A sample of elliptical galaxy profiles. Visual surface brightness arcsec^{-2} is plotted against the log of the radius in arc seconds. Solid lines are fits of eq. (8) to the data.

Two attempts to improve on Hubble's law which have been popular are de Vaucouleurs's (1948) law

$$\log S = \log S_0 - 3.25[(r/\beta)^{1/4} - 1], \qquad (6)$$

and the family of models calculated by King (1966) for globular clusters. The weakness of de Vaucouleurs's law is that it has only two free parameters, for length and surface brightness scales; the shape is fixed. Comparison with the observations shows that while it fits the profiles of some galaxies fairly well, many others either have too pronounced an r^{-2} power law

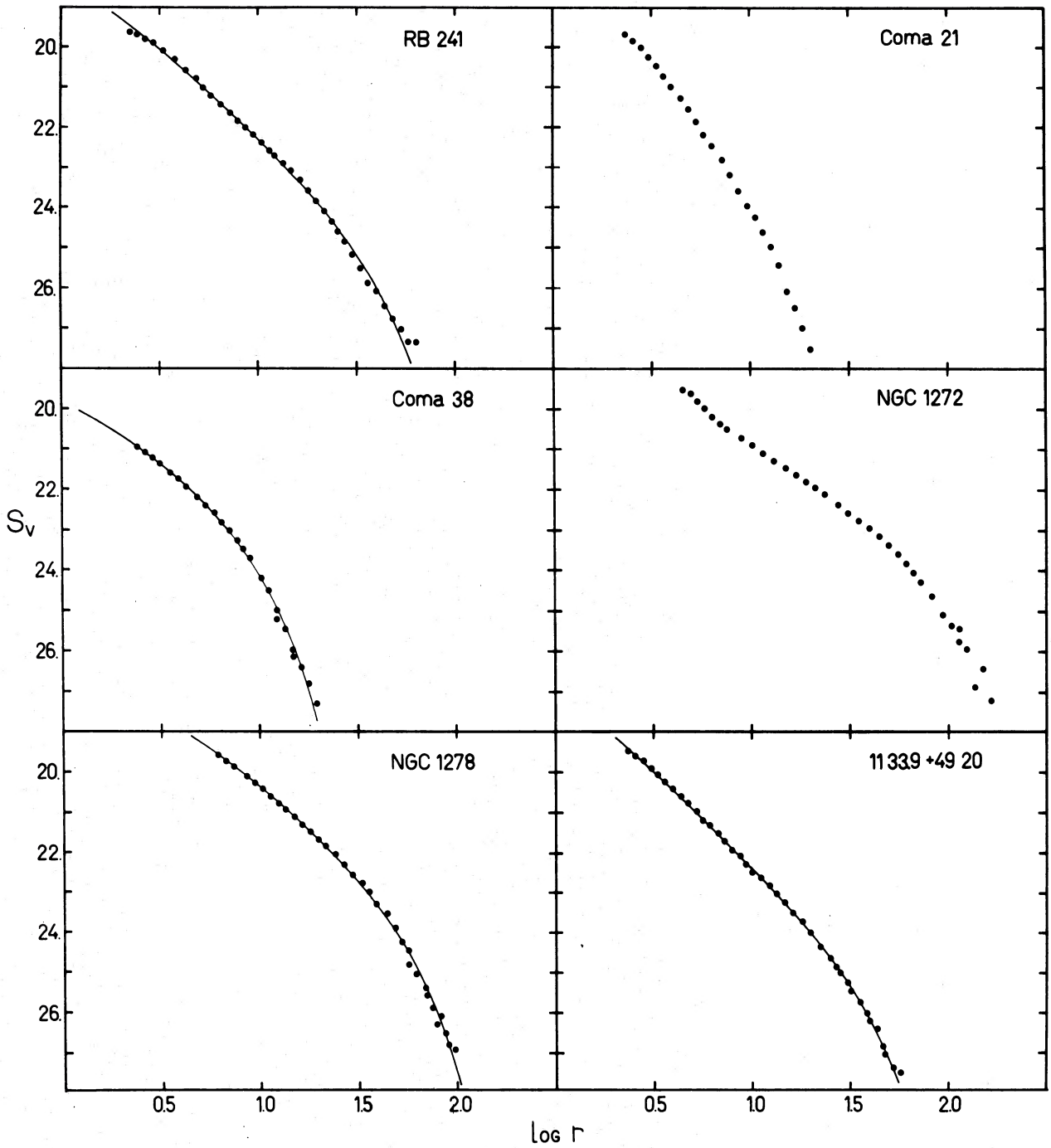

FIG. 4.—*Continued*

section or have envelopes which are too severely truncated for this law. King's models work much better, giving excellent fits to most small galaxies and also to some large galaxies such as NGC 4816 and NGC 4841 whose profiles contain a slight inflection. However, the profiles of many large galaxies do have an extended r^{-2} segment, described well by Hubble's law but not by the King models, which tend toward an isothermal r^{-1} projected light distribution.

An additional inconvenience of King's models is that they cannot be represented by a simple analytic formula. A little experimenting turned up a simple

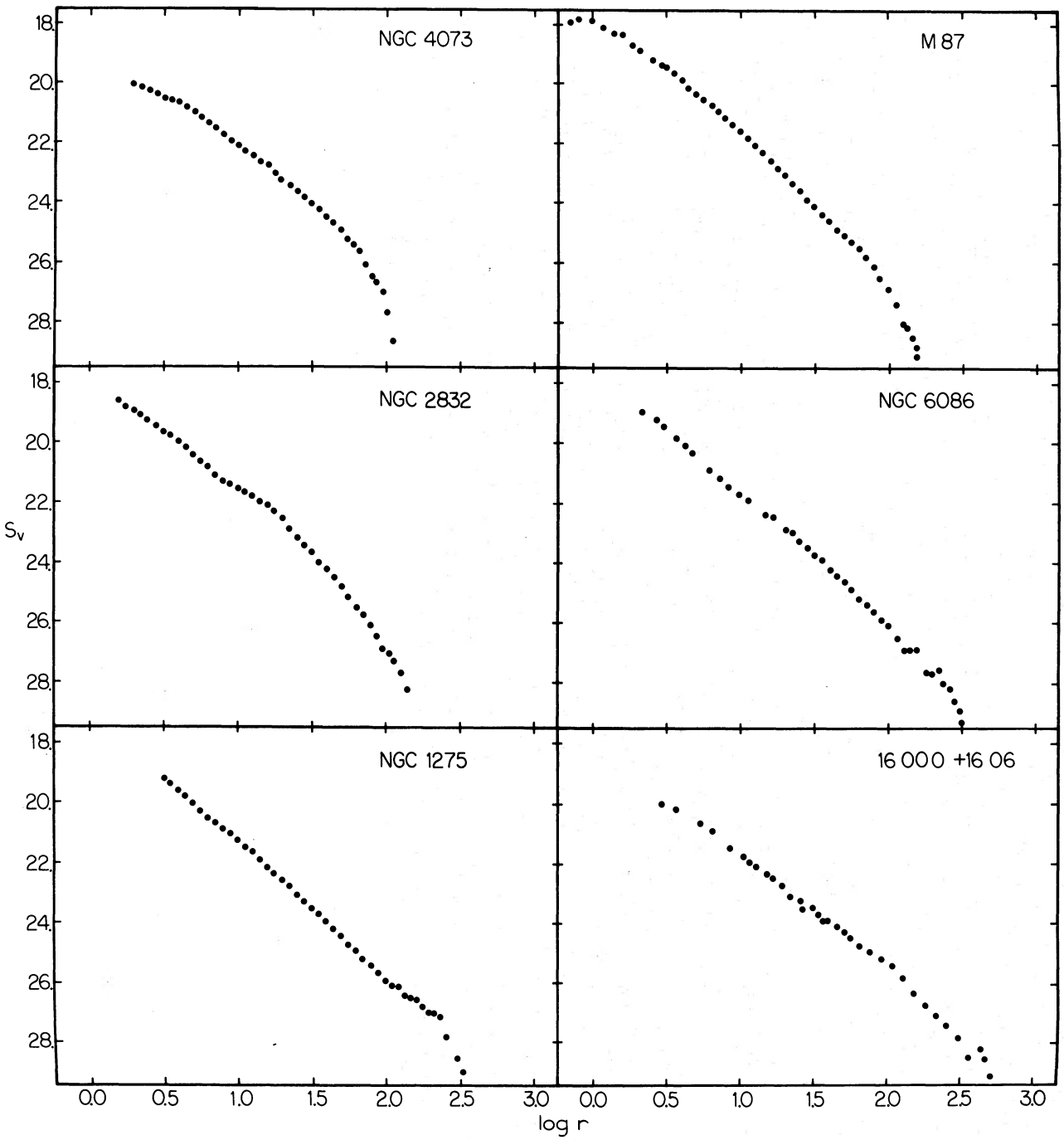

FIG. 5.—Profiles of brightest cluster members. Visual surface brightness arcsec^{-2} is plotted against the log of the radius in kpc.

expression which does fit the profiles of most elliptical galaxies quite well. It is a Hubble law modified by an exponential cutoff of the form

$$S = \frac{S_0 \exp\left[-(r/\alpha)^2\right]}{(1 + r/\beta)^2} . \qquad (7)$$

The solid lines through the points in Figure 4 are fits of this formula to the data. In fitting the profiles of galaxies for which the core radius β is not well determined, it is convenient to transform the expression to a form in which the parameters are more nearly dependent,

$$S = \frac{I_0 \exp\left[-(r/\alpha)^2\right]}{(r + \beta)^2} . \qquad (8)$$

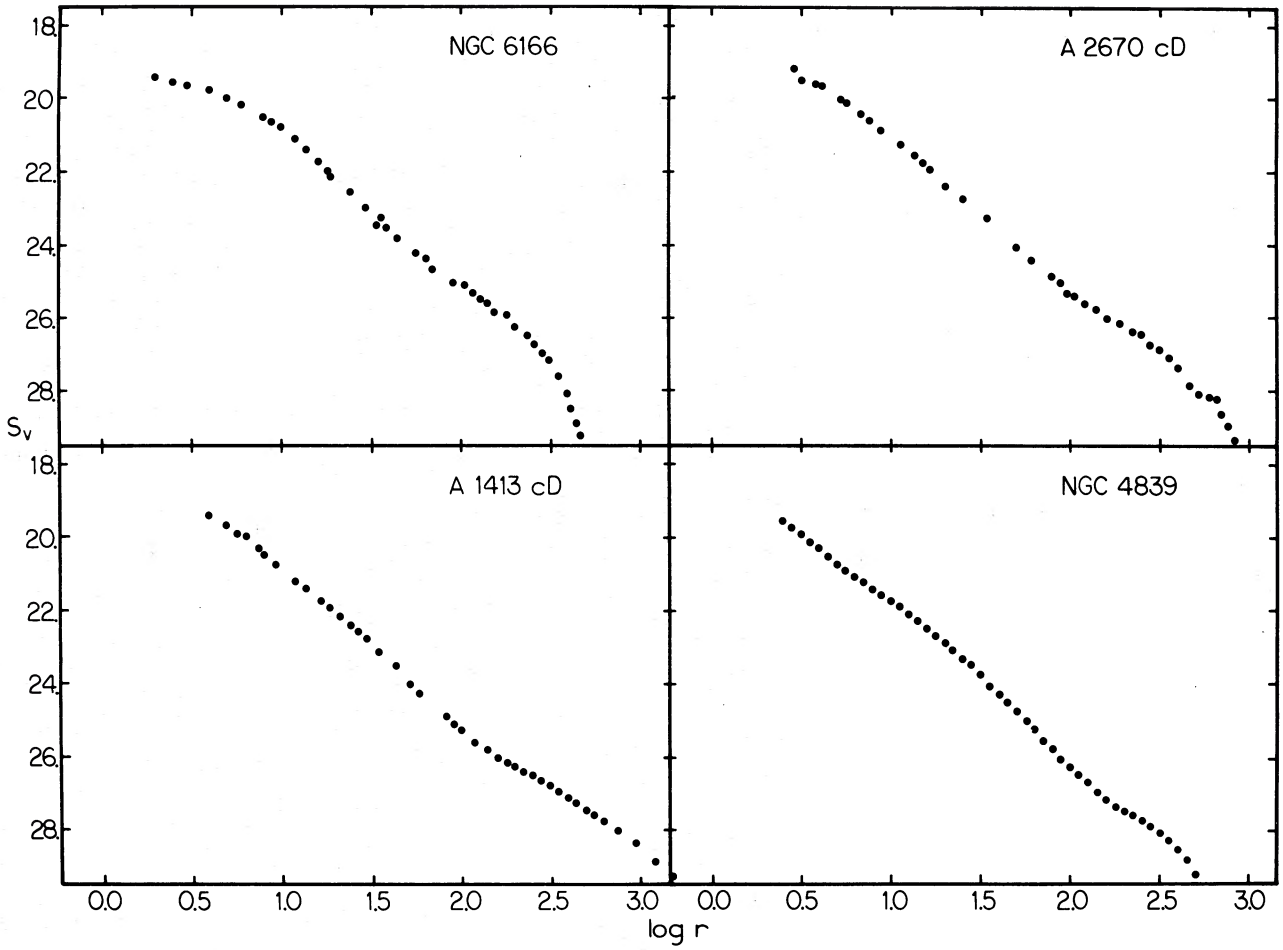

FIG. 5.—*Continued*

Note that $I_0 = S_0\beta^2$ is an intensity, and that the total luminosity of the galaxy

$$I = I_0 f(\alpha/\beta)\,, \qquad (9)$$

where, typically, $1 < f < 25$. This convenient number, I_0, which characterizes the power law section of the galaxy profile and is independent of core or envelope size, will be called the *reduced luminosity*; and M_0, the corresponding magnitude, will be called the *reduced magnitude*.

The results of fitting this formula to the observations are tabulated in Tables 1–3. If values are given for all three parameters, it may be assumed that χ^2 for the fit was of order unity per degree of freedom. A few galaxies could not be fitted satisfactorily by equation (8), but were by a King model. These are listed in Table 4 along with the King model parameters: S_0,

TABLE 3

BRIGHTEST CLUSTER MEMBERS

Cluster	Galaxy	M_v	M_0	log α	log β	log R_1	log L_{01}
MKW 4.....	NGC 4073	−23.13	−20.27	...	0.58	2.07	12.10
Perseus.....	NGC 1275	−24.27	−20.66	...	...	2.54	12.46
Virgo.....	M87	−23.53	−20.21	2.13	0.10	2.20	12.27
A779.....	NGC 2832	−23.65	−20.24	...	0.11	2.16	12.31
A1413.....	...	≤ −26.02	−21.37	...	0.46	≥3.30	12.91
A2147.....	1600.0+1606	−24.43	−20.54	...	0.55	2.68	...
A2162.....	NGC 6086	−23.95	−20.29	...	...	2.51	12.41
A2199.....	NGC 6166	−24.89	...	...	...	2.67	12.76
A2634.....	NGC 7728	−24.5	−20.59	...	...	...	12.67
A2670.....	...	−25.23	−21.04	...	0.45	2.93	12.74

TABLE 4

GALAXIES BEST FITTED BY A KING MODEL

Galaxy	M_0'	log r_t	log r_c
NGC 4816.....	−18.94	2.43	0.19
NGC 4841.....	−19.64	2.16	0.13
NGC 4957.....	−19.19	2.09	0.09
IC 842.....	−17.79	1.74	−0.26
1300.4+28 07.....	−16.89	1.10	0.10
RB 195.....	−16.83	1.13	0.14
RB 268.....	−17.29	1.99	−0.26
Coma 25.....	−16.92	1.36	0.09
3 15.6+41 34.....	−18.54	1.57	0.22
3 16.2+21 27.....	−19.59	1.66	0.36

the central surface brightness; r_t, the tidal radius; and r_c, the core radius. All lengths in Tables 1–4 are in kiloparsecs. A very few galaxies could not be fitted satisfactorily with either family of profiles. Some, like NGC 4816, are probably misclassified S0's; some are simply peculiar.

It must be stressed that no physical significance is claimed for either of these fitting methods. For our purposes, both may be regarded as quantifiable families of French curves, convenient for describing the light distribution in a galaxy with a few numbers. Even though a particular curve fits a galaxy profile well over the observed range in radius, the parameters of the curve may be quite unrelated to the true structure of the galaxy. In particular, the King model parameters, S_0 and r_c, of small galaxies are very uncertain and are no more likely than many other pairs of possible values.

The cutoff radius R_1 is also listed in Tables 1–3, for those galaxies with adequate photometry. In most cases this was determined by visually estimating the radius where the rapidly dropping brightness profile would reach zero. Comparison of these radii with the values of log r_t determined from the fit of a King model envelope to the galaxies shows log R_1 to be smaller by typically 0.15. Thus R_1 is probably systematically low, but it has been used in preference to a fitted r_t because it represents less of an extrapolation from the observed data.

The relation between the cutoff-radius R_1 and the reduced absolute magnitude M_0 of the galaxies in Tables 1–3 is presented in Figure 6. Ellipticals are plotted as filled circles and brightest cluster members as open circles. With the exception of NGC 4839, of the two lower limits, and of the two smallest galaxies, the elliptical galaxies display a quite tight correlation between R_1 and M_0. If the five divergent points are excluded, the least-squares solution is

$$\log R_1 = -0.258\,(12.40 + M_0) \qquad (10)$$

with a dispersion about this relation, $\sigma = 0.14$. Converting to luminosity, this may be expressed, within the uncertainties, as

$$R_1 \sim L_0^{2/3}\,. \qquad (11)$$

The two lower limits refer to two rather curious galaxies, IC 3957 and IC 3959. The profile of IC 3957 is shown in Figure 4; that of IC 3959 is quite similar. Both are r^{-2} power laws, with no sign of either a core or an outer cutoff. These two galaxies are located 1′ apart about 15′ SW of the center of the Coma cluster. Their visual appearance is perfectly normal. Their recessional velocities, as reported by Gregory (1975), are close to the mean velocity of the cluster. Other than their proximity, they appear to have nothing in common which distinguishes them from the other ellipticals in Coma. NGC 4839, the other discrepant bright galaxy, will be discussed in detail in § IV*c*.

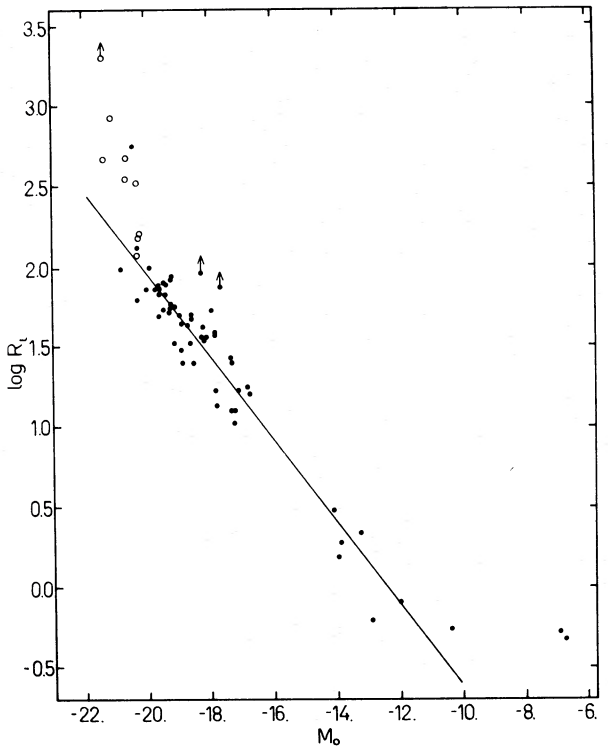

FIG. 6.—The log of the limiting radii of galaxies (in kpc) versus their absolute reduced magnitudes. Open circles are brightest cluster members.

How much of the rather small scatter in log R_1 is real? It is difficult to reliably determine the error in log R_1, but a reasonable guess would be $\sigma = 0.08$, somewhat smaller than the observed dispersion. A number of authors (Gallagher and Ostriker 1972; Richstone 1974; Biermann and Silk 1975) have suggested that encounters between cluster galaxies may result in substantial tidal stripping of their outer envelopes. The observed dispersion in R_1 provides a means of testing this hypothesis. Figure 7 presents the relation between the environment of Coma cluster galaxies and the truncation of their envelopes. The deviation of log R_1 from the mean relation in Figure 6 is plotted, for each galaxy, against its projected distance, in arc minutes, from the cluster center. The slope of Δ log R_1 versus r, determined from a least-squares fit excluding the two lower limits, is -0.002 ± 0.004. Thus there is no evidence that galaxies in the

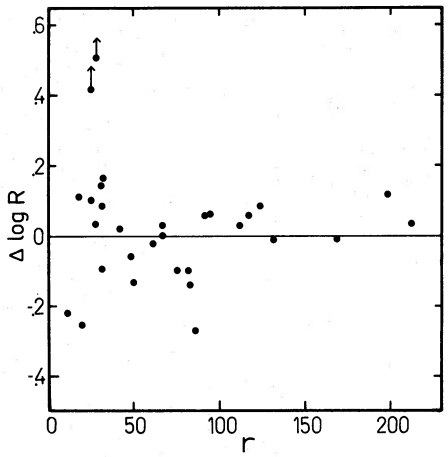

FIG. 7.—Deviation of Coma ellipticals from the solid line in Fig. 6 versus their projected distance (in arcmin) from the cluster center.

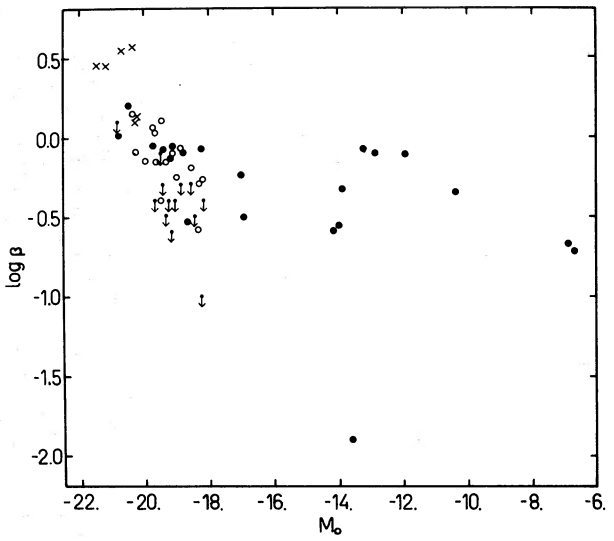

FIG. 8.—The log of the core radii of galaxies (in kpc) versus their absolute reduced magnitudes. *Filled circles*, galaxies in Table 2; *open circles*, galaxies in Table 1; *crosses*, brightest cluster members.

center of Coma, which have suffered more encounters than galaxies in the outer parts, have less extended envelopes than the latter.

The small scatter about the mean relation also argues against the importance of tidal encounters in determining the present sizes of galaxies. Since the typical galaxy could have experienced only a few disruptive encounters since formation one would expect a very wide range of tidal cutoffs. It should be noted that, since all but the two smallest dwarf ellipticals also obey equation (10), there is no justification in assuming, as is often done in analogy to the globular clusters, that their outer radii were determined by encounters with the Galaxy or M31.

The inner scale length, β, is much more poorly determined than the outer cutoff. The most reliable data available on the variation of β with M_0 are presented in Figure 8. Nearby galaxies from Table 2 are represented by filled circles; brightest cluster members, by $\times$'s. Data on galaxies in Table 1 are the least reliable, because of their distance. Only data on those galaxies with $M_0 < -18$ are plotted, as open circles and upper limits. Despite the poor quality of the data, one can discern an obvious trend. Core radius decreases with decreasing luminosity but makes a sudden jump at $M_0 \approx -14$, equivalent to $M_{\rm tot} \approx -15$. The qualitative fact that galaxies fainter than M32 lack small cores has, of course, been noticed before. Larson (1974*b*) has recently suggested that this change is due to the inability of small galaxies to hold on to their interstellar gas against the disruptive force of supernova explosions during formation.

No mention has been made, so far, of one additional observed parameter of galaxies: their ellipticity. Ellipticity was not given much attention in this study because most of the galaxies studied were almost round ($1.0 > b/a > 0.8$) and because it is the least reliably determined quantity with this photometry method. An attempt to find correlations between ellipticity and other galaxy parameters was not successful. Ignoring ellipticity, and considering the uncertainties in the data, both R_1 (or α) and β are sufficiently well correlated with M_0 to justify considering elliptical galaxies to be members of a one-parameter family.

b) Brightest Cluster Members

The most striking characteristic of the brightest cluster members, whose profiles are presented in Figure 5, is their enormous extent—greater than 2 Mpc in the case of A1413. Their profiles also display a wider variety of shapes than do the cluster ellipticals. With the exception of M87, none could be fitted to either a truncated Hubble law or to one of the King models. The smallest galaxies appear to be the least abnormal. The larger galaxies tend to have envelopes with gradients smaller than r^{-2}, a trend which in the most extreme cases of A2670 and A1413 results in an inflection and distinct hump in the outer envelope.

In general, the light distribution of the inner parts is similar to that of a normal giant elliptical. In fact, whether it is physically meaningful or not, one can decompose these profiles into that of a normal elliptical plus an extended low-surface-brightness halo. One striking exception is NGC 6166, whose core is of considerably lower central surface brightness than that of a normal large galaxy.

That the envelopes of the brightest cluster members are too extended for normal ellipticals can be seen in Figure 6, where their limiting radii are plotted as open circles. Although there are few normal ellipticals with reduced magnitudes as bright as those of the brightest cluster members, it seems clear that the latter do not represent the extension of the normal elliptical sequence to larger objects. It would be a remarkable coincidence if the relation between R_1 and M_0 which is obeyed by ellipticals over a brightness

range of 10^4 should suddenly change at precisely the magnitude of brightest cluster members.

The core radii of brightest cluster members may be compared with those of normal galaxies in Figure 8, where the former are plotted as ×'s. Although the most extreme brightest cluster members seem to have very large cores, the data are too poor to tell whether they are anomalously large for galaxies of that brightness.

The brightest cluster members display a wide range of properties, from near normal to extremely abnormal. A comparison of the galaxy properties with the total luminosities of the clusters in which they are found shows that the degree of abnormality is not random. Cluster luminosities are listed in the last column of Table 3. Those of A1413, A2199, and A2670 are taken from Oemler (1974); that of Virgo comes from Abell (1972). The total luminosity of MKW 4 was found by integrating the brightness of those cluster members measured by Zwicky *et al.* (1961–1968) and applying a correction factor for faint galaxies in the manner described in Oemler (1974). The luminosities of the other clusters were crudely estimated using a relation between luminosity, distance, and the number of cluster members found by Zwicky *et al.* which was established using the clusters in Oemler (1974). These values are rather uncertain.

The relation between total galaxy magnitude and total cluster luminosity is plotted in Figure 9 as filled circles. Considering the uncertainties in the latter quantity, the correlation is remarkably good. Roughly, $L_{\rm gal} \approx L_{\rm cl}^{1.25}$. The very bright magnitudes and the strong dependence on cluster luminosity are due, of course, to the extended outer envelopes of the cD galaxies. The envelope-independent reduced magnitudes of the same galaxies are shown in Figure 9 as open circles. Note that galaxy luminosity still increases with cluster luminosity, but at a much slower rate.

We may use the reduced magnitudes to predict the total luminosities which the brightest cluster members would have if they did not have abnormally extended envelopes. The relation between M_0 and $M_{\rm tot}$ for normal bright ellipticals is presented in Figure 10. The mean relation shown by the line in Figure 10 has been used to produce the total magnitudes shown as ×'s in Figure 9. These may be compared with the solid line, which represents the relation between $M_{\rm tot}$ and $L_{\rm cl}$ predicted by Schechter (1976) from the luminosity functions in Oemler (1974), with the assumption that $M_J(24.1) - M_V({\rm tot}) = 0.55$. The half-magnitude difference between the points and the line reflects the obvious fact that even the centers of cD galaxies are anomalously bright. What was not obvious before is that even apparently normal brightest cluster members such as M87 and NGC 6086 are also exceptionally luminous. If Schechter's predicted relation is shifted up by 0.5 mag to the position of the dashed line, the derived magnitudes follow with an rms scatter of only 0.11 mag. For comparison, Sandage (1972*b*) finds a dispersion of all brightest cluster members of 0.25 mag. One must conclude that the brightest members of elliptical rich clusters form a very homogeneous class of objects whose reduced luminosities depend on cluster luminosity in the way predicted by the assumption of a universal galaxy luminosity function.

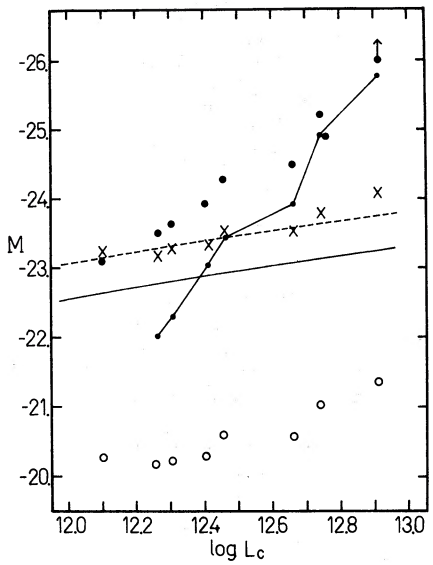

FIG. 9.—The magnitudes of brightest cluster members versus the luminosity of their clusters. See § IV*b*.

The differences between the ×'s and the filled circles in Figure 9 are due to the extended envelopes of the cD's. This excess luminosity is plotted as connected dots and is a very strong function of cluster luminosity.

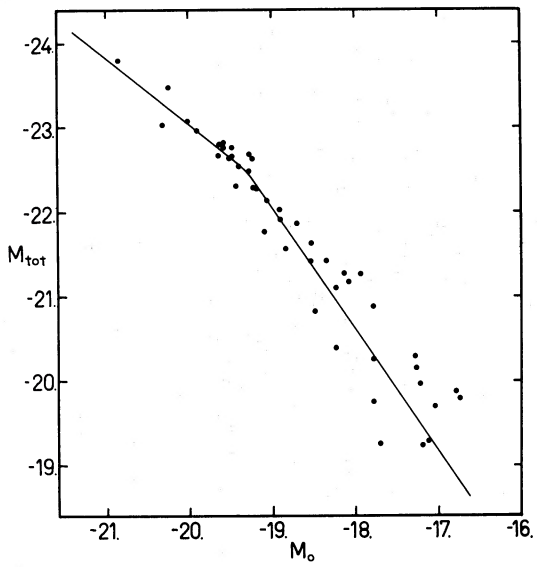

FIG. 10.—The relation between reduced and total magnitudes of bright normal ellipticals.

Roughly,

$$L_{\rm env} \approx L_{\rm cl}^{2.2} . \quad (12)$$

c) NGC 4839

The discussion above has ignored the odd case of NGC 4839, which has the properties of a misplaced brightest cluster member. It has as extended a halo as the typical cD galaxy; and the shape of its profile, including the characteristic hump near the outer edge, closely resembles cD galaxies like that in A2670. However, it is not the brightest, or even second brightest, member of a cluster, nor is it located in the center of a cluster, as all other cD galaxies are (see Fig. 3).

There is no question that it is a member of the Coma cluster, rather than being the brightest member of a small background cluster. Its recessional velocity of 7455 km s^{-1} differs by only $\frac{1}{2}\sigma$ from the mean (6967 km s^{-1}) of Coma (Gregory 1975), and the mean velocity of galaxies within a projected radius of 1 Mpc differs from that of the entire cluster by only 63 $\pm$ 164 km s^{-1}. Nor is there any evidence for a clustering of galaxies around NGC 4839. Nothing except its great size distinguishes it from any other member of the Coma cluster.

Unless and until it can be explained away, NGC 4839 remains a counter example to the general rule that cD galaxies are always the centrally located, brightest members of clusters of galaxies, a rule which has important implications for theories of the origin of cD's.

V. DISCUSSION

It has been shown above that normal elliptical galaxies form a very homogeneous class of objects from which brightest cluster members differ substantially. It is not clear how many of the latter objects should be called cD galaxies. According to the original definition, a cD is a galaxy with an extended halo which is the outstandingly bright member of a cluster of galaxies. All of the objects studied above meet the second requirement, but only those in the more populous clusters meet the first. Instead of discussing cD galaxies, it might be more illuminating to define the *cD phenomenon. Among clusters of galaxies, there exists a subset whose brightest members have exceptionally bright cores. These galaxies possess, in addition, extended halos whose total luminosity is a strong function of cluster richness.*

There appear to be two separate phenomena occurring here. The excessively bright reduced magnitudes of these galaxies seem to be a function only of cluster morphology: in the terminology of Oemler (1974) all of the objects studied came from either cD or extreme spiral-poor clusters. The second phenomenon, the extended envelopes, seems to be tied in a particularly intimate way to processes in the cluster as a whole. Several possibilities for such a process have been suggested recently. Gallagher and Ostriker (1972), Oemler (1973), and Richstone (1974) have suggested that the envelopes are simply intergalactic trash: material torn from the outer envelopes of cluster members by tidal interactions and now moving in the potential well of the cluster. Unfortunately, the lack of evidence for tidal stripping of galaxies, discussed above, seriously weakens this theory.

Alternatively, Lecar (1975), White (1975), Ostriker and Tremaine (1975), and others have explored the effects of dynamical friction on the relaxation process in clusters. Large galaxies falling to the cluster center and being torn apart by their mutual tidal forces would produce an intergalactic medium of stars similar to that formed by the envelope stripping process. White has calculated models of such a process in the isothermal core of a cluster like Coma. For an assumed *galaxy* mass-luminosity ratio of 100 (Turner 1975), his model predicts an excess luminosity equal to -25.85 visual mag. Comparison with Figure 9 at $L_c = 9.4 \times 10^{12} L_\odot$ shows a remarkable agreement with the observations. However, it is not clear whether the model can predict the $L_c^{2.2}$ dependence of envelope luminosity. The fractional increase in central cluster density in White's model is a function of core size and central density. Inspection of the lists of core radii and densities for cD and spiral-poor clusters in Bahcall (1975) reveals no real trend of either with cluster luminosity, suggesting a constant evolution rate and $L \approx L_c^{1.0}$. However, the data, especially on core densities, have considerable scatter. Also, what is really needed is *initial* core radii and densities which may be quite different from present values. Thus, it is impossible to quantitatively judge the model's predictions yet.

Both of the above models depend on cluster-wide processes. A galaxy initially located at the cluster center is simply a lucky bystander; the envelope it collects about itself does not really belong to it: the galaxy and the diffuse halo both simply reside at the bottom of the same potential well. Thus, there is no reason why the diffuse component should necessarily have a giant elliptical galaxy at its center. NGC 6166 is a possible example of this situation; its outer parts are typical of cD's, but its core seems much too diffuse to be the core of a giant elliptical galaxy.

Neither of these theories, however, can explain the case of NGC 4839, which has the properties of a cD but which does not sit at the bottom of the potential well of the Coma cluster. Ostriker and Tremaine have also proposed a variation of the dynamical friction model that can. In this model, a large galaxy captures passersby by the gravitational drag of the large galaxy's envelope on the passing galaxy. Although most effective at the center of a cluster, this process can operate anywhere and thus could explain the case of NGC 4839. It is not yet clear whether its quantitative predictions match the observations.

I am very grateful to Drs. James Gunn and Stephen Shectman for their help with plate material, data, and advice during this work. Many of the observations were made while the author was a Virginia Steele Scott Fellow at the California Institute of Technology.

REFERENCES

Abell, G. O. 1972, in *IAU Symposium 44, External Galaxies and Quasi-stellar Objects*, ed. D. S. Evans (Dordrecht: Reidel), p. 341.
Ables, D. A., and Ables, P. G. 1972, *A.J.*, **77**, 642.
Bahcall, N. A. 1975, *Ap. J.*, **198**, 249.
Biermann, P., and Silk, J. 1975, preprint.
Burkhead, M. S., and Kalinowski, J. K. 1974, *A.J.*, **79**, 835.
de Vaucouleurs, G. 1948, *Ann. d'Ap.*, **11**, 247.
———. 1953, *M.N.R.A.S.*, **113**, 134.
———. 1969, *Ap. Letters*, **4**, 17.
Gallagher, J. S., and Ostriker, J. P. 1972, *A. J.*, **77**, 288.
Gott, J. R. 1975, *Ap. J.*, **201**, 296.
Gregory, S. A. 1975, *Ap. J.*, **199**, 1.
Gunn, J. E., and Oke, J. B. 1975, *Ap. J.*, **195**, 255.
Hodge, P. W. 1961, *A.J.*, **66**, 384.
———. 1962, *A.J.*, **67**, 125.
———. 1963*a*, *A.J.*, **68**, 470.
———. 1963*b*, *A.J.*, **68**, 691.
———. 1964*a*, *A.J.*, **69**, 438.
———. 1964*b*, *A.J.*, **69**, 853.
———. 1973, *Ap. J.*, **182**, 671.
———. 1974, Circular 12, IAU Comm. 28.
Hodge, P. W., and Smith, D. W. 1974, *Ap. J.*, **188**, 19.
Hubble, E. 1930, *Ap. J.*, **71**, 231.
Jones, W. B., Obitts, D. L., Gallett, R. M., and de Vaucouleurs, G. 1967, *Pub. Dept. Astr. Univ. Texas at Austin*, Ser. 2, Vol. **1**, No. 8.
King, I. R. 1966, *A.J.*, **71**, 64.
Kormendy, J., and Bahcall, J. N. 1974, *A. J.*, **79**, 671.
Larson, R. B. 1974*a*, *M.N.R.A.S.*, **166**, 585.
———. 1974*b*, *M.N.R.A.S.*, **169**, 229.
Lecar, M. 1975, in *IAU Symposium 69, Dynamics of Stellar Systems*, ed. A. Hayli (Dordrecht: Reidel), p. 161.
Liller, M. H. 1960, *Ap. J.*, **132**, 306.
Liller, M. H. 1966, *Ap. J.*, **146**, 28.
Markaryan, B. E., Oganesyan, E. Y., and Arakelyan, S. N. 1965, *Astrophysics*, **1**, 23.
Matthews, T. A., Morgan, W. W., and Schmidt, M. 1964, *Ap. J.*, **140**, 35.
Miller, R. H., and Prendergast, K. H. 1962, *Ap. J.*, **136**, 713.
Minkowski, R. 1961, *A.J.*, **66**, 558.
Morgan, W. W. 1958, *Pub. A.S.P.*, **70**, 364.
Morgan, W. W., Kayser, S., and White, R. A. 1975, *Ap. J.*, **199**, 545.
Morgan, W. W., and Lesh, J. R. 1965, *Ap. J.*, **142**, 1364.
Noonan, T. W. 1973, *A.J.*, **78**, 26.
Oemler, A. 1973, *Ap. J.*, **180**, 11.
———. 1974, *Ap. J.*, **194**, 1.
Ostriker, J. P., and Tremaine, S. D. 1975, preprint.
Peterson, B. A. 1970, *A.J.*, **75**, 695.
Richstone, D. O. 1974, unpublished Ph.D. thesis, Princeton University.
Rood, H. J., and Baum, W. A. 1967, *A.J.*, **72**, 398.
———. 1968, *A.J.*, **73**, 442.
Sandage, A. R. 1961, *Ap. J.*, **133**, 355.
———. 1972*a*, *Ap. J.*, **170**, 1.
———. 1972*b*, *Ap. J.*, **278**, 1.
———. 1972*c*, *Ap. J.*, **178**, 25.
———. 1973, *Ap. J.*, **183**, 711.
Schechter, P. 1976, *Ap. J.*, **203**, 297.
Turner, E. L. 1975, unpublished Ph.D. thesis, California Institute of Technology.
van Houten, C. J. 1961, *B.A.N.*, **16**, 1.
White, S. D. M. 1975, preprint.
Wilson, C. P. 1975, *A.J.*, **80**, 175.
Zwicky, F., Herzog, E., Wild, P., Karpowicz, M., and Kowal, C. 1961–1968, *Catalogue of Galaxies and Clusters of Galaxies* (Pasadena: California Institute of Technology).

Note added in proof.—I have been informed by Dr. F. Bertola that the discrepancy in the last point of Baum's data in Figure 2 is due to a misprint in Liller (1966). The first parameter in Table 4 is not, as stated in the text, S_0, but rather $M_0' = -2.5 \log (I_0 r_c^2) + C$.

AUGUSTUS OEMLER, JR.: Yale University Observatory, Box 2023 Yale Station, New Haven, CT 06520